

The New Ternary Ceramics of MAX Phases, the Solution of All Obstacles (Theoretical and Experimental Review)

Dr. Ahmed M. H. Abdulkadhim Al-Ghaban 

Materials Engineering Department, University of Technology/Baghdad

Email:ahmed_gaban@yahoo.com

Received on: 30/10/2012 & Accepted on: 9 / 5/2013

ABSTRACT

In the recent years the new ternary carbides or nitrides materials with the formula of $M_{n+1}AX_n$ where M is a transition metal, A is an element from group IIIA or IVA, X is either Carbon or Nitrogen, and (n=1-3) have been given more attention due to their unusual set of mechanical and physical properties. In this manuscript types, properties and some very new applications of these so called MAX phases in bulk and thin films forms have been reviewed. Some experimental results are also given. This research may shed light on these materials to be candidates for many potential applications.

اطوار السيراميك الثلاثي من ماكس ، الحل لكل العقبات

الخلاصة

في السنوات الاخيرة احتل السيراميك الثلاثي من الكاربيدات والنتريدات ذي الصيغة الكيميائية ($M_{n+1}A_nX_n$) حيث م هو فلز انتقالي و أ هو فلز من المجموعة الثالثة الى المجموعة الثالثة عشر في الجدول الدوري اما س فهو اما الكربون او النيتروجين و ن من واحد الى ثلاثة احتل مكان متميز كمادة هندسية فريدة نسبة الى الخواص الميكانيكية والفيزيائية الغير اعتيادية التي يمتاز بها. في هذا البحث فان انواع وخواص وبعض التطبيقات الحديثة لهذه المواد المدعاة باطوار ال م أس قد تم عرضها في حالة الكتلة والافلام الرقيقة. بعض النتائج العملية ايضا ذكرت. هذا البحث قد يسلم الضوء على هذه المواد لتكون مرشحة لعدة تطبيقات حيوية للمواد الهندسية.

INTRODUCTION

Functional properties of materials, e.g. for automotive and decorative applications, depend often on their surface properties. The major conventional routes to harness these materials against corrosive attack are by passivation or galvanic protection (e.g. coating with metals, e.g. Zinc). Corrosion protection with ceramic coatings is not compatible with post deposition forming or joining processes, because the ceramic coating is expected to fail due to brittle fracture. A new class of ternary ceramic materials [1-4] exhibiting fully reversible plastic deformation while being stable at high temperatures [1-4] has recently received attention. The general formula is $M_{n+1}AX_n$, (n=1-3), where M is a transition metal, A is an element mainly from group IIIA or IVA and X is either C or N. Figure (1) shows the location of M, A and X elements in the periodic table

and the synthesized materials from the three groups of 211, 312 and 413 [2]. Figure 2 shows the ideal crystal structure of MAX phases from three different groups 211, 312 and 413.

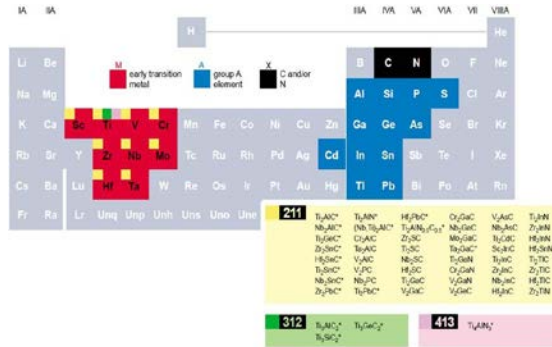


Figure (1) The reported MAX phases and the location of the M, A, and X elements in the periodic table [2].

These, so called MAX phases are thermally and electrically conductive [5, 6], thermal shock resistant, damage tolerant [7], resistant to corrosion and oxidation [8, 9] and quite recently they also found to be radiation tolerant [10]. The origin of these rather unique properties, i.e. a previously unforeseen combination of metallic and ceramic attributes, is due to their nanolaminated atomic arrangement. Bulk MAX phases have been synthesized by sintering a mixture of elements or compounds under isostatic pressure at elevated temperatures [11, 12], by solid-liquid reaction synthesis [13] as well as by mechanically induced self-propagating reaction [14, 15]. Thin films have been grown by magnetron sputtering [4, 16-18], pulsed cathodic arc [19], reactive chemical vapor deposition [20] and pulsed laser deposition was also attempted [21].

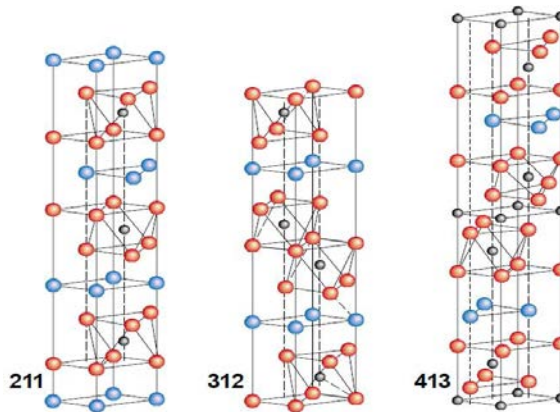


Figure (2) The crystal structure of three different MAX phase systems 211, 312 and 413. The red spheres refer to the M element, the blue to the A element and the black to the X element [2].

The production of phase pure thin films at low temperatures is challenging and the identification of low temperature formation pathways is an active research area for both bulk [22-25] and thin film processing [16,18]. Reducing the bulk synthesis temperature may reduce processing and energy cost [23] while a deposition temperature reduction may allow for the use on temperature-sensitive substrates, such as steel, during thin film processing [16, 18, and 26].

Zhou and Sun [27] proposed the notion that Si intercalation into TiC_x is causing the transformation from cubic TiC_x to hexagonal Ti_3SiC_2 in 2000. In this paper the implications of intercalation for bulk processing of phase pure MAX phases were discussed. Seven years after the intercalation notion was launched by Zhou and Sun [27], Riley and Kisi reported a low temperature synthesis pathway for bulk Ti_3AlC_2 [22, 23] based on intercalation. Ti_3AlC_2 MAX phase was produced at 400-600°C lower temperature as compared with the conventional bulk synthesis temperature by annealing a $\text{TiC}_{0.67}$ -Al powder mixture [22]. It has been argued that the direct ingress of the an element into ordered vacancy sites of milled M_{n+1}X_n caused the formation of the $\text{M}_{n+1}\text{AX}_n$ phase [22]. Theoretical studies support the notion that Al may be incorporated in TiC_x ($x < 1$) and vacancy ordering could take place to form MAX phases at low synthesis temperatures [28, 29]. This scenario is quite similar to the suggested out-diffusion mechanism which is responsible for the decomposition of MAX phase into TiC_x and A element [30]. While this similarity has already been discussed by Zhou and Sun in 2000 [27] experimental reports of intercalation of MAX phases are rare. This may at least in part be due the structural similarity between reactants, possible intermediate reaction products and the MAX Phases resulting in diffraction peak overlaps. In addition the magnitude of possible intermediate reaction products, such as intermetallics, transition metal carbides and nitrides as well as A element carbides and nitrides may complicate the analysis of the diffraction data further. Nevertheless considering the arguments discussed above the intercalation process could - if active - a very promising low temperature synthesis pathway for bulk MAX phases as well as for thin films. Although the synthesis of MAX phases is an active research area, studies of MAX phase formation mechanisms are comparatively rare. Identifying the underlying reaction mechanisms as well as to describe the energetics and kinetics of the MAX phase formation are essential for exploring alternative synthesis pathways including low temperature processes. Hence, the crystallization kinetics of Cr_2AlC and V_2AlC from amorphous MAX phase composition 2:1:1 was investigated.

It has been argued that the low temperature deposition of crystalline Cr_2AlC is enabled by surface diffusion processes [16]. Consistent with [16] the formation of crystalline Cr_2AlC was observed at 500°C by Li et al. [31]. Furthermore, they observed the formation of a triple-layered structure with an α - $(\text{Cr,Al})_2\text{O}_3$ inner layer, an amorphous intermediate layer and a crystalline Cr_2AlC outer layer at 370°C [31]. The later formation of the Cr_2AlC layer was suggested to be due to the raised surface temperature due to thermal barrier properties of the oxide inner layer and the reduced oxygen contamination [31].

The formation of bulk Cr_2AlC on the other hand was reported from elemental powders by hot pressing [32]. DSC and XRD data indicate that as Al starts to melt, an exothermic reaction is observed at 670°C which is related to the formation of $\text{Cr}_9\text{Al}_{17}$ [32]. As the temperature is increased further several intermetallic phases form until at 1050°C the formation of Cr_2AlC is observed by reaction of Cr,

graphite, AlCr_2 and Al_8Cr_5 [32]. Recently, Li et al. reported the formation of bulk Cr_2AlC by mechanically activated hot-pressing technology at 1100°C [23]. Hence, the temperature range of $1050\text{--}1100^\circ\text{C}$ appears to be required for the synthesis of bulk Cr_2AlC [32, 33].

In bulk form Gupta et al. [34] synthesized V_2AlC by reactive hot isostatic pressing at 1600°C for 8 h. Furthermore, single crystals of V_2AlC were formed in metallic melts at a temperature range of $1500\text{--}1600^\circ\text{C}$ [35]. VAl_3 , V_7Al_{45} and VAl_{10} were additionally identified in the final products [35]. Recently, the formation of V_2AlC was observed during hot pressing a powder of V, Al and C at $T \geq 900^\circ\text{C}$ [36]. Phase pure V_2AlC was reported in the temperature range of $1400\text{--}1600^\circ\text{C}$. The reaction between Al_8V_5 and C was identified to be responsible for the V_2AlC formation [36].

Growth of V_2AlC thin film was reported in 2006 by Schneider et al. [37] utilizing sputtering from three elemental targets at 850°C substrate temperature. Sigumonroung et al. [38] reported that the threshold temperature range for single phase V_2AlC formation lies between 650 and 750°C . At lower growth temperatures the formation of hexagonal V_2C , Al_8V_5 and Al_3V was observed [38]. Scabarozzi [39] reported the epitaxial formation of V_2AlC by combinatorial sputtering on c-axis sapphire, using VC and TiC buffer layers and substrate temperature between 575 and 900°C .

EXPERIMENTAL PART

The first part of this project focuses on the formation of Ti_2AlC and Ti_3AlC_2 MAX phases from cubic TiC_x ($0.4 \leq x \leq 1$) and Al. The influence of the C content and the annealing temperature on the phase formation of TiC_x/Al sputtered bilayers after annealing in vacuum is studied systematically. Furthermore, the potential of the bilayer annealing procedure as a low temperature synthesis pathway for MAX-phase thin films was explored and discussed. TiC_x/Al bilayer thin films were synthesized using combinatorial magnetron sputtering. Based on energy dispersive X-ray analysis (EDX) calibrated by elastic recoil detection analysis data, x in TiC_x was varied from 0.4 to 1.0. The film constitution was studied by X-ray diffraction before and after annealing at temperatures from 500 to 1000°C . The formation of TiC_x and Al in the as-deposited samples over the whole C/Ti range was identified. Upon annealing TiC_x reacts with Al to form Ti-Al based intermetallics. Already at 700°C the formation of MAX phases (space group P63/mmc) is observed at $x \leq 0.7$. Based on the comparison between the C content induced changes in the lattice spacing of TiC_x and Ti_2AlC as well as Ti_3AlC_2 , the direct formation of MAX phases by Al intercalation into TiC_x for $x \leq 0.7$ was inferred.

Figure (3) represents the formation of Ti_2AlC and Ti_3AlC_2 MAX phases at different annealing temperatures.

Here an evidence for the direct formation of Ti_2AlC by Al intercalation into TiC_x ($x \leq 0.7$) in the x range of $0.4 \leq x \leq 0.5$ is provided. This conclusion is enabled by the here adopted combinatorial experimental strategy where the effect of x in TiC_x of the reactant material on the phase formation upon annealing was studied by XRD in the x range of 0.4 to 0.5.

In the second part it is attempted to describe the energetics and kinetics of the MAX phase formation which are essential for exploring alternative synthesis pathways including low synthesis temperature processes.

On this basis the formation kinetics of crystallization of Cr_2AlC and V_2AlC MAX phases were investigated by differential scanning calorimetry (DSC) and X-ray diffraction (XRD). Amorphous Cr_2AlC thin films were produced by magnetron sputtering. Two exothermal peaks are observed during DSC up to 1200 °C. XRD data suggest that the first DSC peak is associated with the formation of hexagonal $(\text{Cr,Al})_2\text{C}_x$, while according to the second DSC peak Cr_2AlC is formed. The activation energy for the phase transformations are 426 and 762 kJ/mol, respectively.

Figure (4) represents the formation of Cr_2AlC MAX phase based on the DSC temperatures.

On the third part V_2AlC thin film previously sputtering was amorphous as prepared. The crystallization kinetics were investigated by differential scanning calorimetry (DSC) and X-ray diffraction (XRD). During continuous heating up to 1200 °C, one exothermal peak is observed between 565 and 675 °C. XRD data suggest that the DSC peak is associated with the formation of V_2AlC (prototypes Cr_2AlC , space group P63/mmc). The activation energy of crystallization of V_2AlC is ~ 308 kJ/mol based on the Kissinger approach. This value is close to the activation energy of 287 kJ/mol obtained as for the transformation of magnetron sputtered hexagonal $(\text{V,Al})_2\text{C}_x$ thin films to V_2AlC . The here reported phase formation temperature of V_2AlC is about 800 K lower than during hot pressing of elemental powders.

Figure (5) represents the formation of V_2AlC MAX phases due to the DSC temperatures.

CONCLUSIONS

Although the synthesis of MAX phases is an active research area, studies of MAX phase formation mechanisms are comparatively rare. Identifying the underlying reaction mechanisms as well as to describe the energetics and kinetics of the MAX phase formation are essential for exploring alternative synthesis pathways including low synthesis temperature processes.

In this work the phase stability of three different MAX phase thin film systems, namely Ti-Al-C, Cr-Al-C, and V-Al-C, is investigated.

The first part shows that the x in TiC_x ($x \leq 0.7$) influences the structure of the product formed. TiC_x/Al bilayer thin films were synthesized using combinatorial magnetron sputtering to study the influence of the C content on the reaction products at different annealing temperatures. Based on EDX calibrated by ERDA, x in TiC_x was varied from 0.4 to 1.0. The film constitution was studied by XRD before and after annealing at temperatures range (500 to 1000) °C. The formation of TiC_x and Al in the as-deposited samples in the whole x range was identified by XRD. At $x < 1$ TiC_x reacts with Al to form the Ti-Al based intermetallics at $T \leq 700^\circ\text{C}$. At 700 °C, the formation of MAX phases is observed in a phase mixture with $x \leq 0.7$. At $x \sim 0.5$, Ti_2AlC is the most dominant phase beside the residual TiC in the temperature range $\geq 800^\circ$. Based on the comparison between the C content induced changes in the lattice parameter of TiC_x and d -spacing of Ti_2AlC (10-13), (11-20), (20-23), and (11-26) as well as Ti_3AlC_2 (10-14), (11-20), (11-28), and (20-24), the direct formation of MAX phases by Al intercalation into TiC_x for $x \leq 0.7$ was inferred.

In the second part, the ambition is to shed light on the mechanisms responsible for the formation of crystalline Cr_2AlC and V_2AlC by studying the formation kinetics. Hence, amorphous Cr_2AlC thin films were produced by magnetron sputtering. The crystallization kinetics of Cr_2AlC were investigated by differential scanning calorimetry (DSC) and X-ray diffraction (XRD). Two exothermal peaks are observed during DSC up to 1200 °C. XRD data suggest that the first DSC peak is associated with the formation of hexagonal $(\text{Cr,Al})_2\text{C}_x$, while according to the second DSC peak, Cr_2AlC is formed. The activation energy for the phase transformations are 426 and 762 kJ/mol, respectively. Both transformations appear to be diffusion controlled. The formation of Cr_2AlC occurs at a temperature of about 440 °C lower than during hot pressing.

X-ray detect amorphous V_2AlC thin films as well as hexagonal $(\text{V,Al})_2\text{C}_x$ were deposited by magnetron sputtering from a compound target with V_2AlC composition. Differential scanning calorimetry (DSC) and X-ray diffraction (XRD) were employed to characterize the reaction kinetics. During continuous heating up to 1200°C an exothermal peak is observed between 565 and 675°C, depending on the heating rate employed. XRD data suggest that the DSC peak is associated with the formation of hexagonal V_2AlC (prototypes Cr_2AlC , space group $\text{P6}_3/\text{mmc}$). Based on the Kissinger approach the measured activation energy for the formation of V_2AlC from amorphous V_2AlC is 308 kJ/mol, while the activation energy for the reaction of hexagonal $(\text{V,Al})_2\text{C}_x$ to V_2AlC is 287 kJ/mol. Bulk diffusion is suggested to be responsible for the formation of V_2AlC at a temperature about 800°C lower than during hot pressing of elemental powders.

REFERENCES

- [1]. Barsoum, M.W. Prog. Solid St. Chem, 28 (2000) 201-208.
- [2]. Barsoum, M.W. T. El-Raghy, American scientist, 89 (2001) 334-343.
- [3]. Music, D. J.M. Schneider, JOM 59 (2007) 60-64.
- [4]. Eklund, P. M. Beckers, U. Jansson, H. Högberg, L. Hultman, Thin Solid Films 518 (2010) 18511878.
- [5]. Hettinger, J.D. S.E. Lofland, P. Finkel, T. Meehan, J. Palma, K. Harrell, S. Gupta, A. Ganguly, T. El-Raghy, M.W. Barsoum, Phys. Rev. B 72 (2005) 115120-115120-6.
- [6]. Barsoum, M.W. T. El-Raghy, J. Am. Ceram. Soc. 79 (1996) 1953-1956.
- [7]. Tzenov, N.V.M.W. Barsoum, J. Am. Ceram. Soc. 83 (2000) 825-832.
- [8]. El-Raghy, T. A. Zavaliangos, M.W. Barsoum, S.R. Kalidindi, J. Am. Ceram. Soc. 80 (1997) 513-516.
- [9]. Sun, Z. Y. Zhou, M. Li, Acta Mater. 49 (2001) 4347-4353.
- [10]. Whittle, K.R. M.G. Blackford, R.D. Aughterson, S. Moricca, G.R. Lumpkin, D.P. Riley, N.J. Zaluzee, Acta Mater. 58 (2010) 4362-4368.
- [11]. Zhou, AC. Wang, Y. Huang, Mater. Sci. Eng. A 352 (2003) 333-339.
- [12]. Khoptiar, Y. I. Gotman, E.Y. Gutmanas, J. Am. Ceram. Soc. 88 (2005) 28-33.
- [13]. Zhou, Y. Y. Sun, S. Chen, Y. Zhang, Mat. Res. Innov. 2 (1998) 142-146.
- [14]. S.-B. Li, H.-X. Zhai, G.P. Bei, Y. Zhou, Z.L. Zhang, Mater. Sci. Technol. 22 (2006) 667-672.
- [15]. Hendaoui, A. D. Vrel, A. Amara, P. Langlois, M. Andasmas, M. Guerioune, J. Eur. Ceram. Soc. 30 (2010) 1049-1057.

- [16]. Walter, C. D.P. Sigumonrong, T. El-Raghy, J.M. Schneider, *Thin Solid Films* 515 (2006) 389-393.
- [17]. Walter, C. C. Martinez, T. El-Raghy, J.M. Schneider, *Steel Res. Int.* 76 (2005) 225-228.
- [18]. Wilhelmsson, O. P. Eklund, H. Högberg, L. Hultman, U. Jansson, *Acta Mater.* 56 (2008) 2563-2569.
- [19]. Rosén, J. L. Ryves, P.O. Å Persson, M.M.M. Bilek, *J. Appl. Phys.* 101 (2007) 101-102.
- [20]. Fakih, H. S. Jacques, M.-P. Berthet, F. Bosselet, O. Dezellus, J.-C. Viala, *Surf. Coat. Technol.* 201 (2006) 3748-3355.
- [21]. Lange, C. M. W. Barsoum, P. Schaaf, *Appl. Surf. Sci.* 254 (2007) 1232-1235.
- [22]. Riley, D. P. E.H. Kisi, *J. Am. Ceram. Soc.* 90 (2007) 2231-2235.
- [23]. Riley, D. P. E.H. Kisi, *J. Aust. Ceram. Soc.* 43 (2007) 102-109.
- [24]. Han, J.H.S.S. Hwang, D. Lee, S.W. Park, *J. Eur. Ceram. Soc.* 28 (2008) 979-988.
- [25]. Yang, C.S.Z. Jin, B. Y. Liang, S.S. Jia, *J. Eur. Ceram. Soc.* 29 (2009) 181-185.
- [26]. Rester, M. J. Neidhardt, P. Eklund, J. Emmerlich, H. Liungcrantz, L. Hultman, C. Mitterer, *Mater. Sci. Eng. A* 429 (2006) 90-95.
- [27]. Zhou, Y. Z. Sun, *Mat. Res. Innovant.* 3 (2000) 286-291.
- [28]. Music, D. D.P. Riley, J.M. Schneider, *J. Eur. Ceram. Soc.* 29 (2009) 773-777.
- [29]. Music, D. H. Kölpin, M. to Baben, J.M. Schneider, *J. Eur. Ceram. Soc.* 29 (2009) 2885-2891.
- [30]. Emmerlich, J. D. Music, P. Eklund, O. Wilhelmsson, U. Jansson, J.M. Schneider, H. Högberg, L. Hultman, *Acta Mater.* 55 (2007) 1479-1488.
- [31]. J.J. Li, L.F. Hu, F.Z. Li, M.S. Li, Y. C. Zhou, *Surf. Coat. Technol.* 204 (2010) 3838-3845.
- [32]. Z. Lin, Y. Zhou, M. Li, J. Wang, *Z. Metallkd.* 96 (2005) 291-296.
- [33]. S.B. Li, W.B. Yu, H.X. Zhai, J.M. Song, W. G. Sloof, S. van der Zwaag, *J. Euro. Cer. Soc.* 31 (2011) 217-224.
- [34]. S. Gupta, M.W. Barsoum, *J. Electrochem. Soc.* 151 (2004) D24-D29.
- [35]. Etzkorn, J. M. Ade, H. Hillebrecht, *Inorg. Chem.* 46 (2007) 7646-7653.
- [36]. C. Hu, L. He, M. Liu, X. Wang, J. Wang, M. Li, Y. Bao, Y. Zhou, *J. Am. Ceram. Soc.* 91 (2008) 4029-4035.
- [37]. Schneider, J.M. R. Mertens, D. Music, *J. Appl. Phys.* 99 (2006) 013501-1-013501-1-013501-4.
- [38]. D. Sigumonrong, J. Zhang, Y. Zhou, D. Music, J.M. Schneider, *J. Phys. D: Appl. Phys.* 42 (2009) 185408 (8pp).
- [39]. Scabarozzi, T.H. Jr. (2009). *Combinatorial Investigation of Nanolaminate Ternary Carbide Thin Films.*

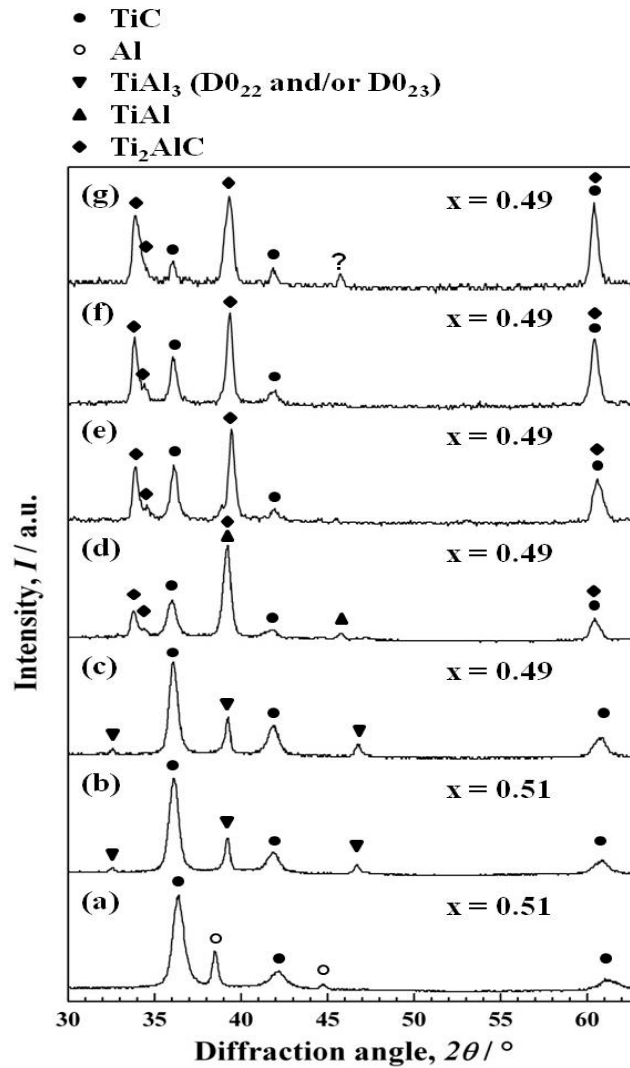


Figure (3) The structural evolution of TiC_{0.5}/Al bilayer thin films for the as-deposited sample (a) and the annealed samples at: (b) 500 °C (c) 600 °C, (d) 700 °C, (e) 800 °C, (f) 900 °C and (g) 1000 °C.

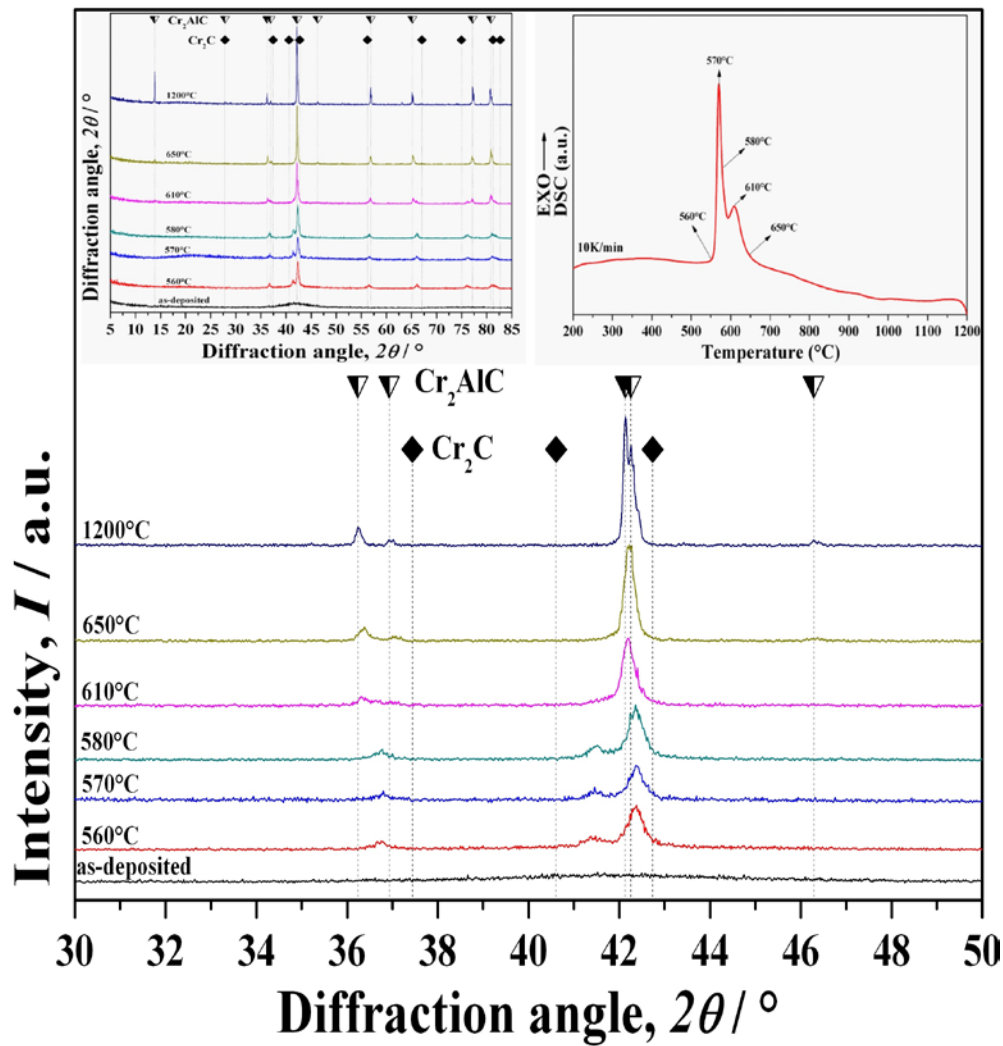


Figure (4) X-ray diffraction data of the as-deposited Cr_2AlC powder together with samples annealed at different temperatures. The inserted curves show the whole XRD 2θ range and the selected temperatures from the DSC measurements with a heating rate of 10 K/min.

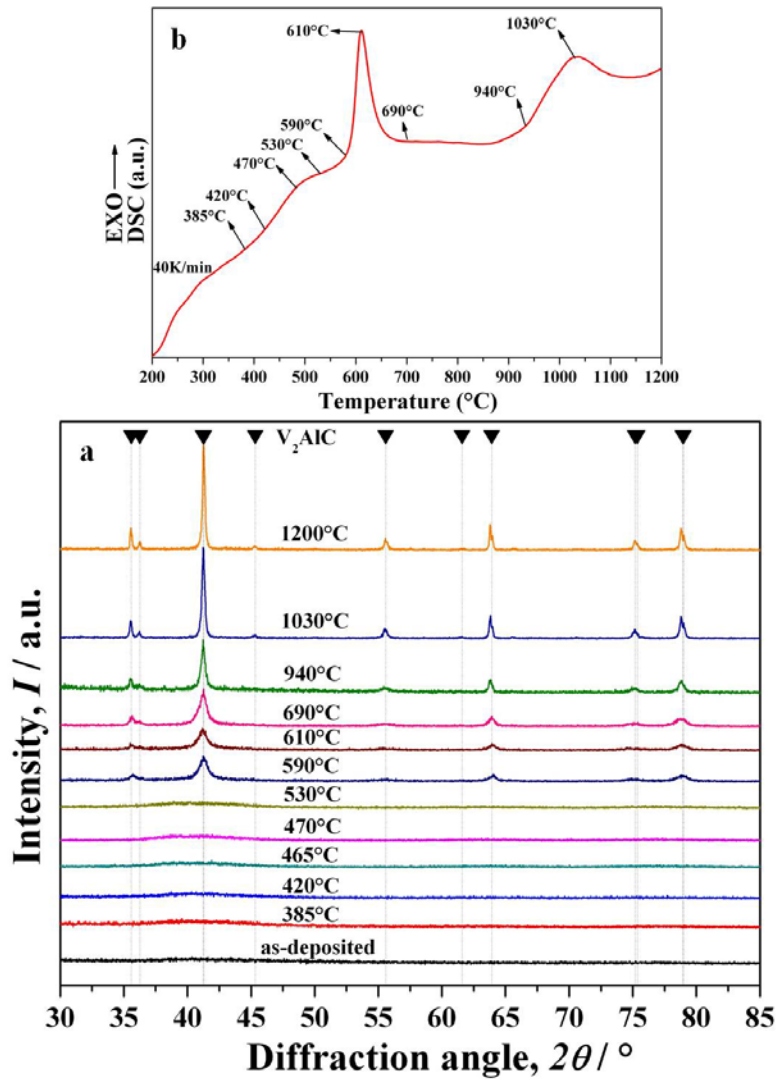


Figure (5) (a) X-ray diffraction data of the as-deposited V_2AlC powder together with samples annealed at different temperatures. (b) The annealing temperatures as selected from the DSC measurements with a heating rate of 40 K/min.